Stability analysis under intrinsic fluctuations: a second-moment perspective of gene regulatory networks

IOP Publishing Phys. Biol. 22 (2025) 066001 https://doi.org/10.1088/1478-3975/ae0b22

Physical Biology

OPEN ACCESS

RECEIVED
30 May 2025

REVISED
12 September 2025

ACCEPTED FOR PUBLICATION
24 September 2025

PUBLISHED
8 October 2025

PAPER

Stability analysis under intrinsic fluctuations: a second-moment perspective of gene regulatory networks

Manuel Eduardo Hernández-García[1], **Mariana Gómez-Schiavon**[2,3] **and Jorge Velázquez-Castro**[1,*]

[1] Facultad de Ciencias Físico Matemáticas, Benemérita Universidad Autónoma de Puebla, Heroica Puebla de Zaragoza, Puebla 72570, Mexico
[2] Laboratorio Internacional de Investigación sobre el Genoma Humano, Universidad Nacional Autónoma de México, Santiago de Querétaro, Querétaro 76230, Mexico
[3] Millennium Science Initiative Program, Millennium Institute for Integrative Biology (iBio), Chilean National Agency for Research and Development, Santiago 8331150, Chile
[*] Author to whom any correspondence should be addressed.

E-mail: jorge.velazquezcastro@correo.buap.mx, manuel.hernandezgarcia@viep.com.mx and mgschiavon@liigh.unam.mx

Keywords: second-moment approach, negative feedback, stochastic dynamics, stability analysis gene regulatory network

Abstract

Gene regulatory networks with negative feedback play a crucial role in conferring robustness and evolutionary resilience to biological systems. However, the discrete nature of molecular components and probabilistic interactions in these networks are inherently subject to fluctuations, which pose challenges for stability analysis. Traditional analysis methods for stochastic systems, like the Langevin equation and the Fokker–Planck equation, are widely used. However, these methods primarily provide approximations of system behavior and may not be suitable for systems that exhibit non-mass-action kinetics, such as those described by Hill functions. In this study, we employed a second-moment approach to analyze the stability of a gene regulatory network with negative feedback under intrinsic fluctuations. By transforming the stochastic system into a set of ordinary differential equations for the mean concentration and second central moment, we performed a stability analysis similar to that used in deterministic models, where there are no fluctuations. Our results show that the incorporation of the second central moment introduces two additional negative eigenvalues, indicating that the system remains stable under intrinsic fluctuations. Furthermore, the stability of the second central moment suggests that the fluctuations do not induce instability in the system. The stationary values of the mean concentrations were found to be the same as those in the deterministic case, indicating that fluctuations did not influence stationary mean concentrations. This framework provides a practical and insightful method for analyzing the stability of stochastic systems and can be extended to other biochemical networks with regulatory feedback and intrinsic fluctuations through a framework of ordinary differential equations.

1. Introduction

Gene regulatory networks inherently exhibit fluctuations owing to the discrete nature of their molecular components and probabilistic interactions among a small number of molecules [1, 2]. Stochastic fluctuations in gene expression arise from both intrinsic and extrinsic sources. Intrinsic fluctuation stems from the random nature of molecular interactions [2, 3], whereas extrinsic fluctuation reflects variability in the cellular environment. Together, these fluctuations can profoundly influence the dynamics and stability of gene networks [4, 5]. Understanding the functional role of such fluctuations is essential because they can lead to adaptive phenotypic variability, for example, through stochastic switching, and may compromise the robustness of biological systems [6].

Various mathematical frameworks have been developed to analyze these stochastic systems. While the chemical master equation provides a general description, it is analytically intractable in most cases [3], leading researchers to employ approximation methods. Among these, the Langevin equation [7], linear noise approximation [8, 9], and Fokker–Planck

equation [3] are widely used. Although some studies have focused on studying gene regulatory networks with negative feedback within a stochastic framework, some of these are based on contrasting what happens with stochastic simulations and with the linear noise approximation [9–11]. However, these methods may be inadequate for systems involving non-mass-action kinetics, such as Hill functions. Hill functions are crucial for modeling cooperative binding and switch-like behavior in gene regulatory networks, capturing the nonlinearity inherent in transcriptional regulation [12]. Moment-based approaches have emerged as powerful alternatives in this context [13, 14]. Hernández-García *et al* [15] established conditions for networks governed by Hill kinetics, under which the second-moment approach precisely describes the system with intrinsic fluctuations. This approach reduces the complexity of the stochastic model to a tractable set of ordinary differential equations describing the mean concentration and second central moment of the molecular species [13, 16]. Although higher-order moments can be incorporated to improve the accuracy [17], the second central moment is often sufficient to capture the essential features of stochastic fluctuations in many biologically relevant systems.

In this study, we leveraged this exact second-moment approach to analyze the stability of gene regulatory networks subject to intrinsic fluctuations. Stability analysis provides insights into the system behavior under perturbations and is critical for understanding the robustness of biological networks. Unlike Lyapunov-based methods, which rely on constructing suitable Lyapunov functions based on approximate stochastic descriptions [18–20], our approach operates directly on the exact moment equations without the need for such approximations. Although other moment-based methodologies utilize the zero-information closure [21] or bounded the value of the moments [22], our approach enables a rigorous stability analysis to be conducted directly from the moment equations. By examining the eigenvalues of the linearized system, we assessed the tendency of the network to return to equilibrium, offering a deeper understanding of how intrinsic fluctuations affect system reliability [23].

To exemplify the approach, we focused on systems with negative feedback, a common regulatory motif in gene networks, which occurs when a gene product inhibits its own production either directly or indirectly [1]. This mechanism acts as a stabilizing force, helping maintain homeostasis and buffer the system against internal and external perturbations [24]. Additionally, this type of system can exhibit oscillations if it has a delay or intermediate processes [25, 26]. Notable examples include the p53-Mdm2 feedback loop [4, 27], in which p53, a tumor suppressor protein, is tightly regulated to prevent uncontrolled cell proliferation, and the Hes-1 system, which plays a key role in neural stem cell differentiation and other developmental processes [28, 29]. Studying such networks is crucial because negative feedback contributes to the robustness, adaptability, and evolutionary resilience of gene regulatory systems [30]. A proper understanding of how stochastic effects interact with feedback mechanisms will be instrumental in unraveling the principles that govern cellular decision-making and stability.

We chose to analyze a gene regulatory network with two nodes and negative feedback as a simple model that appears in diverse biological systems [4, 27–33]. We can find analytic results to compare the differences between deterministic and stochastic stability analyses. We begin by analyzing the deterministic model. Then, using the second-moment approach, we perform a similar stability analysis that considers stochastic effects by introducing ordinary differential equations for the second central moment.

The remainder of this paper is organized as follows. In section 2, we introduce the chemical master equation and derive a set of ordinary differential equations for the mean and second central moment, using the moment-based approach. In section 3, we focus on the stability analysis of a gene regulatory network with negative feedback, where we obtain the conditions for stability in the stochastic regime. Finally, in section 4, we present our discussion and conclusions.

2. Moment approach

First, we present the chemical master equation considering only intrinsic fluctuations. This formulation is fundamental for describing stochastic chemical systems in which extrinsic fluctuations are not included, as these arise from parameter variability, such as changes in external factors like temperature [4]. For this purpose, we followed the methodology of Gardiner [3] for systems with only intrinsic fluctuations. Let be N chemical species, S_l ($l \in \{1,2,\ldots,N\}$) and m reactions $\mathcal{R}_i$ ($i \in \{1,2,\ldots,m\}$), where the species is transformed as follows:

$$\mathcal{R}_i : \sum_{l=1}^{N} \alpha_{il} S_l \xrightarrow{k_i} \sum_{l=1}^{N} \beta_{il} S_l.$$

The coefficients α_{il} and β_{il} are non-negative integers, and are stoichiometric coefficients. k_i are the parameters that determine the rate of the reaction $\mathcal{R}_i$. From these, we derive the stoichiometric matrix of the system $\Gamma_{il} = \beta_{li} - \alpha_{li}$ (indexes are exchanged because it is the transpose). Through collisions (or interactions) between different elements, the system evolves according to the law of mass action, and the propensity rates are, [3]

$$a_i(\mathbf{S}) = k_i \prod_{l=1}^{N} \frac{S_l!}{\Omega^{\alpha_{il}}(S_l - \alpha_{il})!}, \tag{1}$$

where the index i corresponds to reactions $\mathcal{R}_i$ and $\mathbf{S} = (S_1, S_2, \ldots, S_N)$. These propensities represent the transition probabilities per unit of time between different system states. $\Omega = N_A V$ defines the system size, where N_A is Avogadro's number 1 mol^{-1}) and V is the volume. Thus, Ω has units of volume per mole and serves to convert molecule counts into molar concentrations or vice versa [34]. From this, we get the chemical master equation,

$$\partial_t P(\mathbf{S}, t) = \Omega \sum_{i=1}^{m} (a_i(\mathbf{S} - \Gamma_i) P(\mathbf{S} - \Gamma_i, t) - a_i(\mathbf{S}) P(\mathbf{S}, t)), \tag{2}$$

where Γ_i represents the ith column of the matrix $\mathbf{\Gamma}$. Equation (2) describes the temporal evolution of the probability of states of the system.

Analyzing the stability of a system directly from the chemical master equation (2) is highly challenging. Consequently, continuous approximations such as the Langevin equation or Fokker–Planck equation are often used [18]. However, these methods only approximate the system behavior and may be inadequate for systems involving non-mass-action kinetics, such as Hill functions. Then, we employed a moment-based approach [13, 16], which represents the system as a set of ordinary differential equations for the mean concentrations and second central moment. Then, a stability analysis can be performed in the same manner as in the deterministic framework (without fluctuations) [23], thereby significantly simplifying the analysis. Before starting, we define the following quantities:

- The mean concentration of chemical species l, $s_l = \frac{\langle S_l \rangle}{\Omega}$.
- The second central moment between the chemical species l_1 and l_2, $M^2_{l_1,l_2} = \frac{1}{\Omega^2}\langle (S_{l_1} - \langle S_{l_1} \rangle)(S_{l_2} - \langle S_{l_2} \rangle) \rangle$, $(l_1, l_2 \in \{1, 2, \ldots, N\})$.

We assume that an analytical function $f(\mathbf{S})$ of the system variables can be expanded using a second-order Taylor expansion around the mean as follows:

$$\begin{aligned}\langle f(\mathbf{S}) \rangle &\approx \left\langle f(\langle \mathbf{S} \rangle) + \sum_{l_1=1}^{N} (S_{l_1} - \langle S_{l_1} \rangle) \frac{\partial f(\langle \mathbf{S} \rangle)}{\partial S_{l_1}} \sum_{l_1=1}^{N} \right. \\ &\quad \left. + \sum_{l_2=1}^{N} \frac{(S_{l_1} - \langle S_{l_1} \rangle)(S_{l_2} - \langle S_{l_2} \rangle)}{2} \frac{\partial^2 f(\langle \mathbf{S} \rangle)}{\partial S_{l_1} \partial S_{l_2}} \right\rangle \\ &= f(\langle \mathbf{S} \rangle) + \sum_{l_1=1}^{N} \sum_{l_2=1}^{N} \frac{C^2_{l_1,l_2}}{2} \frac{\partial^2 f(\langle \mathbf{S} \rangle)}{\partial S_{l_1} \partial S_{l_2}}, \end{aligned} \tag{3}$$

where $\langle \mathbf{S} \rangle = (\langle S_1 \rangle, \langle S_2 \rangle, \ldots, \langle S_N \rangle)$ is the mean state vector and $C^2_{l_1,l_2} = \Omega^2 M^2_{l_1,l_2}$. If function f is a polynomial until order 2, then the expansion in (3) is exact.

To derive the differential equations for the mean concentration and second central moments from the chemical master equation, we considered reactions up to the first order. For the mean concentration, we multiplied the master equation by S_l, calculated the mean, and utilized (3). A similar approach was applied for the second central moments, resulting in the following equations:

$$\begin{aligned} \frac{\partial s_l}{\partial t} &= \sum_{i=1}^{m} \Gamma_{li} k_i R_i(\mathbf{s}), \\ \frac{\partial M^2_{l_1,l_2}}{\partial t} &= \sum_{i=1}^{m} \left(\frac{\Gamma_{l_1 i}\Gamma_{l_2 i} k_i R_i(\mathbf{s})}{\Omega} + \sum_{l_3=1}^{N} \left(M^2_{l_1,l_3}\Gamma_{l_2 i} k_i \right. \right. \\ &\quad \left. \left. \times \frac{\partial R_i(\mathbf{s})}{\partial s_{l_3}} + M^2_{l_3,l_2}\Gamma_{l_1 i} k_i \frac{\partial R_i(\mathbf{s})}{\partial s_{l_3}} \right) \right), \end{aligned} \tag{4}$$

where $\mathbf{s} = (s_1, s_2, \ldots, s_N)$ and $R_i(\mathbf{s}) = \prod_{l=1}^{N} s_l^{\alpha_{ij}}$ are the reaction rates, these reaction rates are exact. With the second central moment, we can quantify the fluctuations. Using these equations, we analyze a particular system in the next section. Equations in (4) are called the second-moment approach and coincide with the linear noise expansion [35].

Hernández-García *et al* [15] (Corollary 1) showed that the system's dynamics can be exactly captured by ordinary differential equations for the mean and second central moment, provided two conditions are met: (i) the system includes only zero- and first-order reactions, and (ii) the rate constants take the functional form $k_i = k_i^* f(\mathbf{s}, \mathbf{M}^2)$, explicitly depending on the mean concentrations and second central moments. These equations correspond to those in equation (4), but with functional parameters.

3. Stability analysis of a gene regulatory network with negative feedback

In this section, we analyze a gene regulatory network with negative feedback (see figure 1). This type of system is known to exhibit either a stable steady state or oscillatory behavior in deterministic descriptions [25, 26]. In the presence of fluctuations, negative feedback is particularly important, as it can confer robustness and evolutionary resilience [30], and reduce fluctuations. Notably, it is also found in diverse biological systems such as p53 and Hes1, key regulators involved in cancer suppression and cell maintenance [4, 27–32]. Together, these features highlight the crucial role of negative feedback in the function and evolution of gene regulatory networks.

In this study, we used a simplified model with two modules, considering only the dynamics of the proteins (see figure 1). The system is described by the following reactions,

$$\left| \begin{matrix} \emptyset \xrightarrow{\gamma_1} P_1 \\ \emptyset \xrightarrow{\gamma_2} P_2 \end{matrix} \right| \left| \begin{matrix} P_1 \xrightarrow{\delta_1} \emptyset \\ P_2 \xrightarrow{\delta_2} \emptyset \end{matrix} \right|$$

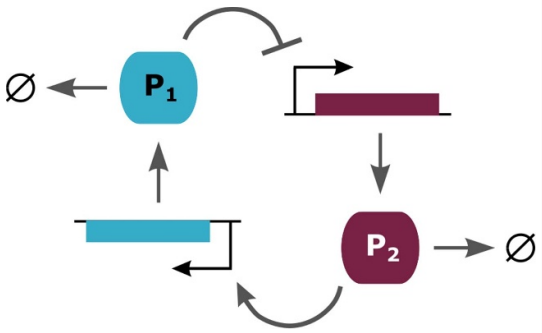

Figure 1. Negative feedback motif. This is a schematic representation of a gene regulatory network with negative feedback, where protein P_1 suppresses the synthesis of protein P_2, whereas P_2 activates the synthesis of P_1, thereby establishing a negative feedback loop. The proteins P_1 and P_2 are degraded.

where the first reaction is the synthesis of P_1, the second is the degradation of P_1, the third is the synthesis of P_2, and the last is the degradation of P_2. Parameters δ_1 and δ_2 are the rates of protein degradation. Without loss of generality, we can take $\delta_1 = \delta$, and $\delta_2 = 1$, which can be shown by variable rescaling. Additionally, the two effective parameters γ_1 and γ_2 are related to the syntheses of P_1 and P_2, respectively, and their forms are given in the following subsections. The stoichiometric coefficients are α_{li} and β_{li}, and the stoichiometric matrix Γ_{il} are,

$$\alpha_{li} = \begin{pmatrix} 0 & 0 \\ 1 & 0 \\ 0 & 0 \\ 0 & 1 \end{pmatrix}, \quad \beta_{li} = \begin{pmatrix} 1 & 0 \\ 0 & 0 \\ 0 & 1 \\ 0 & 0 \end{pmatrix},$$
$$\Gamma_{il} = \begin{pmatrix} 1 & -1 & 0 & 0 \\ 0 & 0 & 1 & -1 \end{pmatrix}. \tag{5}$$

The reaction rates of the system,

$$R_1 = 1, \qquad R_2 = p_1,$$
$$R_3 = 1, \qquad R_4 = p_2. \tag{6}$$

Next, we analyze the system in both deterministic and stochastic regimes, which helps us understand the stability of the system.

3.1. Deterministic stability analysis

First, we analyze the deterministic description of the system. We compared this result with the moment approach, which we present in the next subsection. In this description, the functional parameters γ_1 and γ_2 have the next form,

$$\gamma_1 = \gamma_1^* \left(\frac{\hat{p}_2^2}{1 + \hat{p}_2^2} \right),$$
$$\gamma_2 = \gamma_2^* \left(\frac{1}{1 + \hat{p}_1^2} \right), \tag{7}$$

where $\hat{p}_1$ and $\hat{p}_2$ are the deterministic concentrations of P_1 and P_2 respectively, γ_1^* and γ_2^* are the maximum protein synthesis rates. The terms in parentheses are Hill functions, and we chose the Hill coefficient equal to two for both. The first is the Hill function for an activator and the second for a repressor; thus, we obtain negative feedback. We set the dissociation constant to one in both Hill functions. This is achieved through variable rescaling and reduces the number of parameters in the system. The ordinary differential equations for the deterministic concentrations are

$$\frac{\partial \hat{p}_1}{\partial t} = \gamma_1 - \delta \hat{p}_1,$$
$$\frac{\partial \hat{p}_2}{\partial t} = \gamma_2 - \hat{p}_2. \tag{8}$$

In the stationary state, we need to solve the next equations to get the values of $\hat{p}_{1,ss}$ and $\hat{p}_{2,ss}$

$$0 = \gamma_1^* \left(\frac{(\hat{p}_{2,ss})^2}{1 + (\hat{p}_{2,ss})^2} \right) - \delta \hat{p}_{1,ss},$$
$$0 = \gamma_2^* \left(\frac{1}{1 + (\hat{p}_{1,ss})^2} \right) - \hat{p}_{2,ss}. \tag{9}$$

To do a stability analysis of the system, we need to get a set of differential equations around the equilibrium from (8), where we define

$$\frac{\partial \gamma_1}{\partial \hat{p}_2}|_{(\hat{p}_2 = \hat{p}_{2,ss})} = 2\gamma_1^* \hat{p}_{2,ss} \left(\frac{1}{1 + (\hat{p}_{2,ss})^2} \right)^2 = A_1,$$
$$\frac{\partial \gamma_2}{\partial \hat{p}_1}|_{(\hat{p}_1 = \hat{p}_{1,ss})} = -2\gamma_2^* \hat{p}_{1,ss} \left(\frac{1}{1 + (\hat{p}_{1,ss})^2} \right)^2 = -A_2, \tag{10}$$

defining the next variables as $\Delta\hat{p}_1 = \hat{p}_1 - \hat{p}_{1,ss}$, $\Delta\hat{p}_2 = \hat{p}_2 - \hat{p}_{2,ss}$, the set of ordinary differential equations is as follows:

$$\frac{\partial \Delta\hat{p}_1}{\partial t} = A_1 \Delta\hat{p}_2 - \delta \Delta\hat{p}_1,$$
$$\frac{\partial \Delta\hat{p}_2}{\partial t} = -A_2 \Delta\hat{p}_1 - \Delta\hat{p}_2, \tag{11}$$

then, the Jacobian matrix of this system is

$$J = \begin{pmatrix} -\delta & A_1 \\ -A_2 & -1 \end{pmatrix}. \tag{12}$$

The eigenvalues of this matrix are,

$$\lambda_1 = \frac{1}{2} \left(-1 - \delta + \sqrt{(1-\delta)^2 - 4A_1A_2} \right),$$
$$\lambda_2 = \frac{1}{2} \left(-1 - \delta - \sqrt{(1-\delta)^2 - 4A_1A_2} \right), \tag{13}$$

thus, we can perform a stability analysis because the eigenvalues of the system can be used to determine the stability of the system. The real part of the eigenvalue

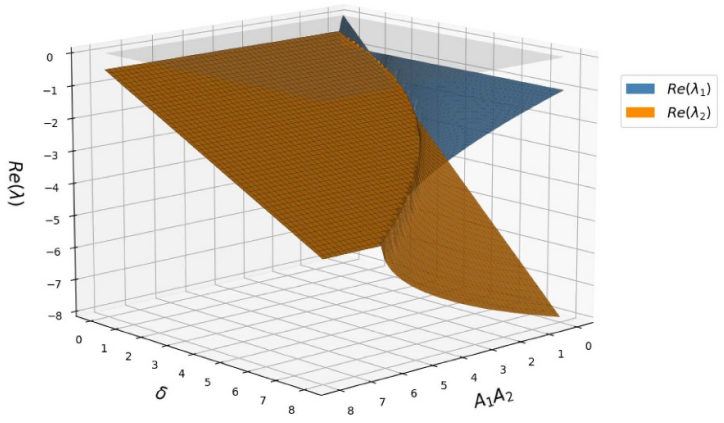

(a) **3D plot**

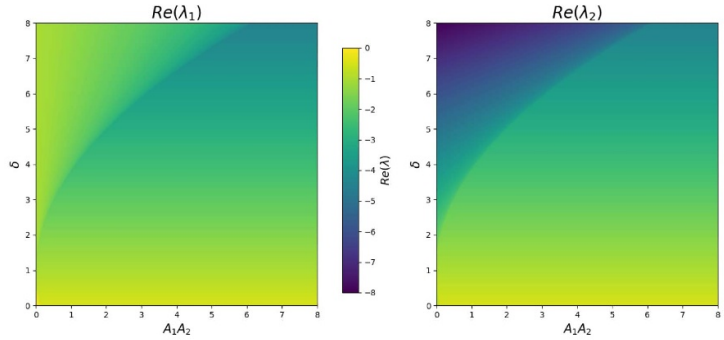

(b) **Contour plot**

Figure 2. Real part of eigenvalues in deterministic regime. We generated both a 3D surface plot and a contour plot to visualize the real parts of eigenvalues. In all cases, the real parts were negative, indicating that the system was stable. Notably, in a particular region of the parameter space, both eigenvalues share equal real parts, whereas their imaginary parts are nonzero. This indicates the presence of damped oscillations because the system exhibits complex eigenvalues with negative real parts in that region.

that dominates the dynamic of the system λ_d determines the stability of the whole system [23], where the eigenvalue that dominates the dynamics is the eigenvalue that has the maximum real part, then:

- If $((1-\delta)^2 - 4A_1A_2) \leqslant 0$:
  then $\mathrm{Re}(\lambda_d) = -\left(\frac{1+\delta}{2}\right)$, in which case the system is stable and has a stable spiral focus, as shown in this region in figure 2, where $\mathrm{Re}(\lambda_1) = \mathrm{Re}(\lambda_2)$.
- If $((1-\delta)^2 - 4A_1A_2) > 0$:
  we analyze this case for cases,
  - if $\delta = 0$ and $A_1A_2 = 0$ then $\lambda_d = 0$, this case does not exist, because if this happens, there is no dynamics in the system.
  - if $\delta \gg 1$ and $\delta \gg A_1A_2$ then $\lambda_d = -\frac{1}{2}$, in this case the system has a stable point.

In figure 2 we show the values of the eigenvalues with respect to δ and A_1A_2, where we can see that the values of the eigenvalues are always minor to zero, the system is always stable when the real parts of both eigenvalues are equal and exhibit damped oscillations, the system has a stable spiral focus, and in the rest of the region, there is a stable point.

3.2. Stochastic stability analysis

In the previous subsection, we analyzed the eigenvalues of the system in a deterministic regime. To perform a similar analysis in the stochastic regime, we propose using a second-moment approach. This method is exact when the system involves only zero- and first-order reactions, and incorporates effective parameters that depend on the second central moment [15], which includes Hill functions. We propose this framework because it describes the stochastic system through a set of ordinary differential equations, thereby simplifying the stability analysis. This reduction is particularly advantageous compared with methods such as Lyapunov functions [18, 19].

In the stochastic regime, the effective parameters γ_1 and γ_2 have the next form,

$$\gamma_1 = \gamma_1^* \left(\frac{\left(p_2^2 + M_{2,2}^2\right) - \frac{p_2}{\Omega}}{1 + \left(p_2^2 + M_{2,2}^2\right) - \frac{p_2}{\Omega}} \right),$$
$$\gamma_2 = \gamma_2^* \left(\frac{1}{1 + \left(p_1^2 + M_{1,1}^2\right) - \frac{p_1}{\Omega}} \right), \qquad (14)$$

where p_1 and p_2 are the mean concentrations of P_1 and P_2, and $M_{1,1}^2$ and $M_{2,2}^2$ are the second central

moments of P_1 and P_2, γ_1^* and γ_2^* are the maximum synthesis rates of the proteins. The terms in parentheses are Hill functions, and we chose the Hill coefficient equal to two for both. For further details on these derivations, please refer to Hernández-García *et al* [15] or appendix A. These Hill functions are exact because they account for all terms without any approximation, including the second central moment. Similar to the deterministic regime, the first Hill function is for an activator, and the second for a repressor. We chose a dissociation constant equal to one for both Hill functions.

This system satisfies Corollary 1 in Hernández-García *et al* [15] and can be described exactly up to the second central moment. Then the equations for the mean concentrations are as follows,

$$\begin{aligned}\frac{\partial p_1}{\partial t} =&\gamma_1 - \delta p_1,\\ \frac{\partial p_2}{\partial t} =&\gamma_2 - p_2,\end{aligned} \tag{15}$$

for the second central moment

$$\begin{aligned}\frac{\partial M^2_{1,1}}{\partial t} =&\frac{1}{\Omega}\left(\gamma_1 + \delta p_1\right) - 2\delta M^2_{1,1},\\ \frac{\partial M^2_{2,2}}{\partial t} =&\frac{1}{\Omega}\left(\gamma_2 + p_2\right) - 2M^2_{2,2}.\end{aligned} \tag{16}$$

The analysis in this work focuses on a specific case, in which the Hill function explicitly depends on the second central moment. However, this framework can be extended to account for higher-order central moments if the Hill function is dependent on these moments [15]. In appendix B, we include an example involving auto-negative regulation, where we show how higher moments behave and how the stability can be affected. Although our main method focuses on second moments, the example illustrates how the framework could be extended.

From (15)–(16), we can analyze the stationary state, then we have the following results for the second central moments,

$$\begin{aligned}M^2_{1,1,ss} =&\frac{p_{1,ss}}{\Omega},\\ M^2_{2,2,ss} =&\frac{p_{2,ss}}{\Omega},\end{aligned} \tag{17}$$

from these results, we see that each protein has a Poisson distribution in the stationary state, in appendix C we compare the results of stochastic simulations and the prediction of equation (17) to the type of distribution. To get the values of $p_{1,ss}$ and $p_{2,ss}$ we need to solve the next equations

$$\begin{aligned}0 =&\gamma_1^*\left(\frac{\left(p_{2,ss}\right)^2}{1+\left(p_{2,ss}\right)^2}\right) - \delta p_{1,ss},\\ 0 =&\gamma_2^*\left(\frac{1}{1+\left(p_{1,ss}\right)^2}\right) - p_{2,ss},\end{aligned} \tag{18}$$

these equations do not depend on the second central moment, and are identical to those employed in the deterministic description to obtain stationary deterministic concentrations. From this result, we can conclude that the moment-based analysis yields the same equations as the deterministic approach for stationary mean concentrations, and fluctuations do not affect the stationary points in accordance with the deterministic description, where fluctuations are absent. Based on (17) and (18), we can find a relation between the determinist concentration and mean concentration, that is, $\hat{p}_1 = \lim_{\Omega\to\infty} p_1$ (similar to protein P_2), where the second central moments (17) are zero, and the size of the fluctuations is zero; in other words, there are no fluctuations.

From (15)–(16) we can get a set of differential equations around the equilibrium, for these we define the next,

$$\begin{aligned}\frac{\partial \gamma_1}{\partial p_2}\Big|_{\left(p_2=p_{2,ss},M^2_{2,2}=\frac{p_{2,ss}}{\Omega}\right)} =&2\gamma_1^* p_{2,ss}\left(\frac{1}{1+\left(p_{2,ss}\right)^2}\right)^2\\ &-\frac{\gamma_1^*}{\Omega}\left(\frac{1}{1+\left(p_{2,ss}\right)^2}\right)^2\\ =&A_1 - \frac{A_3}{\Omega},\\ \frac{\partial \gamma_1}{\partial M^2_{2,2}}\Big|_{\left(p_2=p_{2,ss},M^2_{2,2}=\frac{p_{2,ss}}{\Omega}\right)} =&\gamma_1^*\left(\frac{1}{1+\left(p_{2,ss}\right)^2}\right)^2 = A_3,\\ \frac{\partial \gamma_2}{\partial p_1}\Big|_{\left(p_1=p_{1,ss},M^2_{1,1}=\frac{p_{1,ss}}{\Omega}\right)} =&-2\gamma_2^* p_{1,ss}\left(\frac{1}{1+\left(p_{1,ss}\right)^2}\right)^2\\ &+\frac{\gamma_2^*}{\Omega}\left(\frac{1}{1+\left(p_{1,ss}\right)^2}\right)^2\\ =&-A_2 + \frac{A_4}{\Omega},\\ \frac{\partial \gamma_2}{\partial M^2_{1,1}}\Big|_{\left(p_1=p_{1,ss},M^2_{1,1}=\frac{p_{1,ss}}{\Omega}\right)} =&-\gamma_2^*\left(\frac{1}{1+\left(p_{2,ss}\right)^2}\right)^2 = -A_4,\end{aligned} \tag{19}$$

defining the next variables like $\Delta p_1 = p_1 - p_{1,ss}$, $\Delta p_2 = p_2 - p_{2,ss}$, $\Delta M^2_{1,1} = M^2_{1,1} - M^2_{1,1,ss}$, and $\Delta M^2_{2,2} = M^2_{2,2} - M^2_{2,2,ss}$, then the set of differential equations became like follow, for the mean concentrations

$$\begin{aligned}\frac{\partial \Delta p_1}{\partial t} =&\left(A_1 - \frac{A_3}{\Omega}\right)\Delta p_2 + A_3\Delta M^2_{2,2} - \delta\Delta p_1,\\ \frac{\partial \Delta p_2}{\partial t} =&\left(-A_2 + \frac{A_4}{\Omega}\right)\Delta p_1 - A_4\Delta M^2_{1,1} - \Delta p_2,\end{aligned} \tag{20}$$

for the second central moment

$$\begin{aligned}\frac{\partial \Delta M^2_{1,1}}{\partial t} =&\frac{1}{\Omega}\left(\left(A_1 - \frac{A_3}{\Omega}\right)\Delta p_2 + A_3\Delta M^2_{2,2}\right.\\ &\left.+\delta\Delta p_1\right) - 2\delta\Delta M^2_{1,1},\\ \frac{\partial \Delta M^2_{2,2}}{\partial t} =&\frac{1}{\Omega}\left(\left(-A_2 + \frac{A_4}{\Omega}\right)\Delta p_1 - A_4\Delta M^2_{1,1}\right.\\ &\left.+\Delta p_2\right) - 2\Delta M^2_{2,2},\end{aligned} \tag{21}$$

then, the Jacobian matrix of this system is

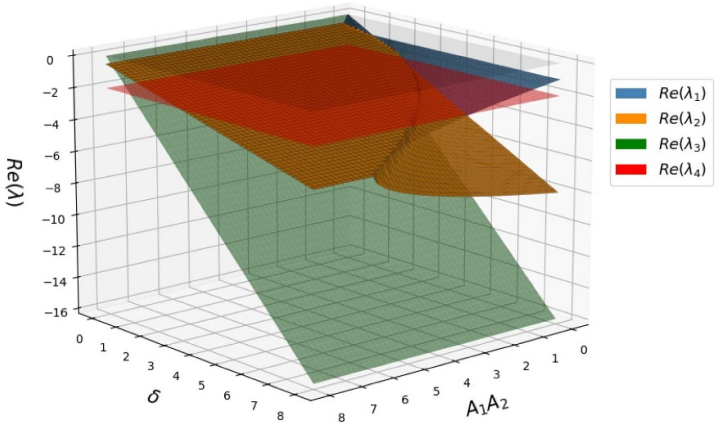

(a) **3D plot**

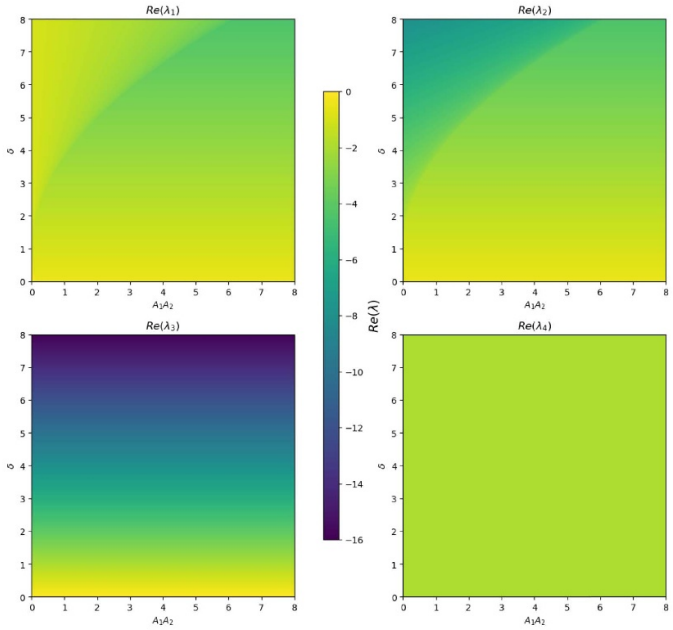

(b) **Contour plot**

Figure 3. Real part of eigenvalues in stochastic regime. We plotted the real parts of the eigenvalues using both a 3D surface plot and a contour plot. The results show that all the real parts of the eigenvalues remain negative, confirming the local stability of the steady state. In particular, we identified a region where two eigenvalues (λ_1 and λ_2) have equal real parts, while their imaginary parts are nonzero, indicating the presence of damped oscillations in this region of the parameter space. Importantly, the eigenvalues do not depend on the system size parameter Ω; therefore, the results of this plot are valid for any system size.

$$J_{sc} = \begin{pmatrix} -\delta & A_1 - \frac{A_3}{\Omega} & 0 & A_3 \\ -A_2 + \frac{A_4}{\Omega} & -1 & -A_4 & 0 \\ \frac{\delta}{\Omega} & \frac{A_1 - \frac{A_3}{\Omega}}{\Omega} & -2\delta & \frac{A_3}{\Omega} \\ \frac{-A_2 + \frac{A_4}{\Omega}}{\Omega} & \frac{1}{\Omega} & -\frac{A_4}{\Omega} & -2 \end{pmatrix}. \quad (22)$$

The eigenvalues of this matrix are

$$\begin{aligned} \lambda_1 &= \frac{1}{2}\left(-1-\delta+\sqrt{(1-\delta)^2 - 4A_1A_2}\right), \\ \lambda_2 &= \frac{1}{2}\left(-1-\delta-\sqrt{(1-\delta)^2 - 4A_1A_2}\right), \\ \lambda_3 &= -2\delta, \\ \lambda_4 &= -2. \end{aligned} \quad (23)$$

It is worth noting that the eigenvalues λ_1 and λ_2 are the same as those obtained in the deterministic regime, and two new eigenvalues, λ_3 and λ_4, appear compared with the deterministic system, which are independent of Ω, the size of the system, and from A_3 and A_4. The case where $\delta = 0$ is discarded because this means that protein P_1 is not degraded. From this, it is evident that both new eigenvalues are less than zero, indicating that the system remains stable under the intrinsic fluctuations captured by the second central moment, and the fluctuations are also stable. In figure 3, all real parts of the eigenvalues of the system are plotted, and we can observe that all are less than zero.

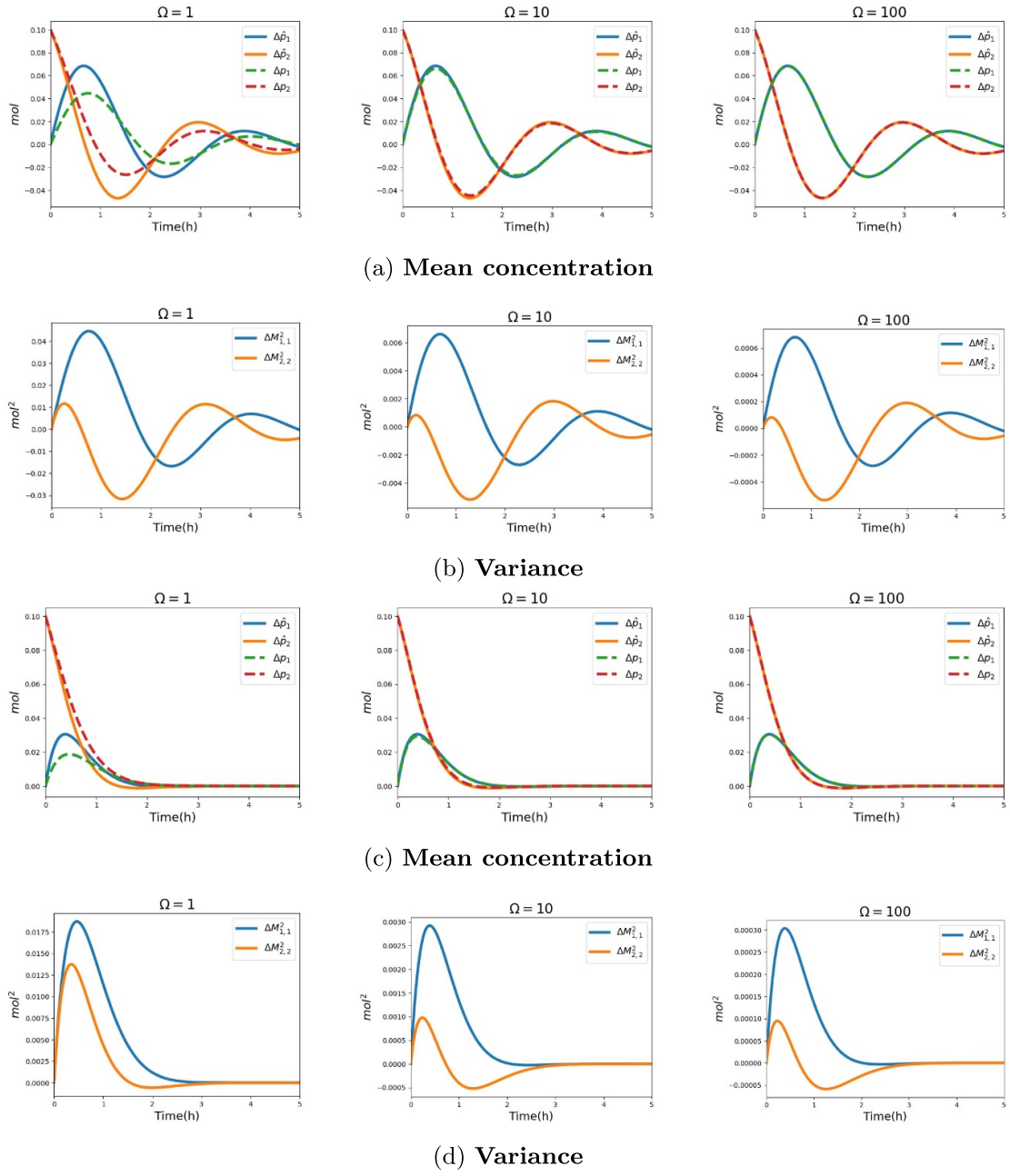

Figure 4. Dynamics of the linearized stochastic and deterministic system under different regimes. We show two representative examples, one of which features a much faster degradation rate for P_1. Panels (a) and (b) correspond to the parameters and initial conditions in table D1, which yield damped oscillations; panels (c) and (d) use the parameters from table D2, where P_1 degrades more rapidly. Panels (a) and (c) compare the deterministic solution $\Delta\hat{p}_1$ with the mean concentration Δp_1 obtained using the second-moment approach, and a similar comparison is made for protein P_2. Panels (b) and (d) show the corresponding variances computed using the second-moment approach. In both cases, we observe that as the system size Ω increases, the mean dynamics approach deterministic behavior, and the magnitude of the second central moment decreases.

Because the eigenvalues λ_3 and λ_4 are independent of the size of the system Ω, we can say that these two eigenvalues are the ones that mainly govern the dynamics of the second central moments, while the first two the mean concentrations. In the system we analyze, the structure of the dynamical equations is independent of the system size Ω, and thus the analytical results are valid for any Ω. However, as shown in figure 4 (where we numerically solved (20)–(21)), the dynamical behavior depends on Ω in practice. For small system sizes (e.g. $\Omega = 1$), the stochastic dynamics deviate noticeably from the deterministic predictions. This discrepancy arises because intrinsic fluctuations introduced through the nonlinear Hill function have a stronger impact on the mean behavior when the molecule numbers are low. In contrast, as Ω increases, the fluctuations diminish, and the stochastic dynamic closely match the deterministic dynamics. This effect is particularly relevant in biological systems, such as gene regulation, where molecule counts are often low and stochastic effects can dominate.

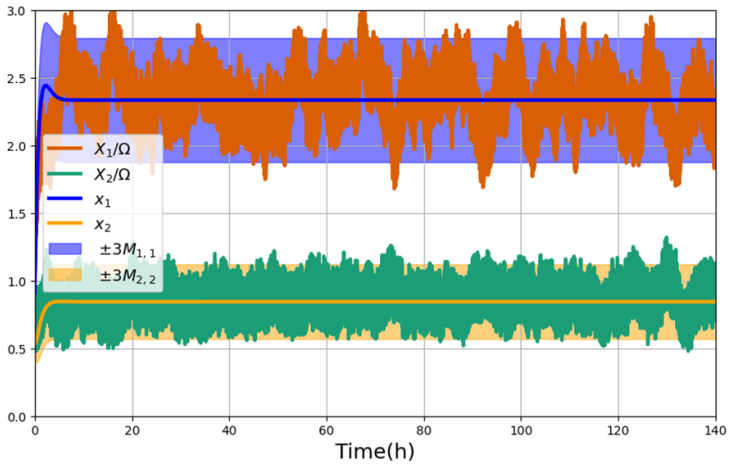

Figure 5. Stochastic simulation vs moment approach. This figure shows the comparison between the stochastic simulations of the model in appendix C (normalized trajectories X_i/Ω) and the predictions obtained from the second-moment approach (16)–(17). Solid curves correspond to the mean concentrations, and shaded regions ($\pm 3M_{i,i}$) indicate the standard deviation. The fluctuations observed in the simulations lie within the predicted variance bands, confirming the accuracy of the moment-based approach. Parameters and initial conditions are listed in table D3.

In figure 5, we compare a stochastic realization of the model described in appendix C with the solution given by the second-moment approach. The fluctuations in the simulation lie within the predicted variance bands. This shows that the moment approach provides an accurate description of both the mean behavior and fluctuations of the stochastic system. Since the system tends to a stationary point, a comparison of stationary distributions (also in C) shows excellent agreement between the stochastic simulations and the second-moment predictions.

Although many existing methodologies for studying gene regulatory networks rely on stochastic simulations or linear noise approximations [9–11], in this study, we employed a set of ODEs that capture the exact dynamics of the system. This approach provides an alternative analytical framework for exploring stochastic behavior by leveraging tools that are traditionally used in deterministic systems. Thus, our methodology offers another perspective for studying intrinsic fluctuations without relying on extensive simulations, potentially facilitating broader analytical insights into the transient dynamics of the gene regulatory networks. This can be relevant for systems such as p53 [4, 27] or Hes-1 [28, 29], where fluctuations can play an important role.

4. Discussion and conclusions

In this study, we performed stability analysis of a gene regulatory network with negative feedback using a second-moment expansion approach. This approach describes the behavior of the system under the assumption that the dynamics emerge from an ensemble of random walks, and captures this behavior through a set of ordinary differential equations for the mean concentration and second central moment.

Traditional stability analysis in a deterministic framework, where fluctuations are absent, is based on studying the stability of a set of ordinary differential equations for deterministic concentrations. However, in this study, we analyzed the stability of a stochastic system affected by intrinsic fluctuations using a set of ordinary differential equations for the mean concentrations and their variance, making the stability analysis of stochastic systems more accessible. Gene regulation was modeled using an exact Hill function that depends on the second central moment. To do this, we used the results from Hernández-García *et al* [15], which allowed us to derive a closed set of differential equations that precisely capture the system's dynamics.

For the specific case studied, the second central moment introduced two additional eigenvalues along with those of the deterministic model. These new eigenvalues were negative, indicating that the system remained stable. Because the deterministic model remains stable for any parameter value, and the additional eigenvalues introduced by the stochastic model are negative, we conclude that intrinsic fluctuations do not compromise the system's stability. Furthermore, the stability of the second central moment suggests that the fluctuations do not induce long-term instability in the system. Additionally, the equations used to determine the stationary values of the mean concentrations were the same as those in the deterministic case, indicating that fluctuations did not alter the stationary state.

The method proposed in this study can be extended to analyze the stability of other biochemical networks, particularly those involving regulatory feedback and intrinsic fluctuations. Moreover, it has potential applications in control theory because it enables the design of control strategies that explicitly

incorporate intrinsic fluctuations, thereby making them more robust to biological variability. This framework enables direct application of control theory techniques developed for ordinary differential equations to stochastic systems.

Data availability statement

No new data were created or analyzed in this study.

Acknowledgments

Manuel E. Hernández-García acknowledges the financial support of SECITHI through the program 'Becas Nacionales 2023'.

Jorge Velázquez-Castro acknowledges financial support of BUAP-VIEP through project 00398-PV.

This work was supported by *Programa de Apoyo a Proyectos de Investigación e Innovación Tecnológica* (PAPIIT UNAM; IA203524 to M.G.-S), and by ANID-Millennium Science Initiative Program-Millennium Institute for Integrative Biology (iBio; ICN17_022 to M.G.-S). Additionally, the authors want to thank for their support to Luis A. Aguilar from the *Laboratorio Nacional de Visualización Científica Avanzada* and Jair Santiago García Sotelo, Iliana Martínez, Rebeca Mucino, and Eglee Lomelín from the *Laboratorio Internacional de Investigación sobre el Genoma Humano, Universidad Nacional Autónoma de México, Santiago de Querétaro, México*.

Declarations

The authors declare no conflicts of interest regarding the publication of this article.

Author contributions

Manuel Eduardo Hernández-García 0009-0007-3090-4392
Conceptualization (equal), Formal analysis (lead), Methodology (lead), Software (lead)

Mariana Gómez-Schiavon 0000-0002-0955-7257
Conceptualization (equal), Methodology (equal), Supervision (equal), Writing – review & editing (equal)

Jorge Velázquez-Castro 0000-0002-7176-2008
Conceptualization (equal), Supervision (equal), Writing – review & editing (equal)

Appendix A. Hill function

In this section, we derive the Hill function that is used in the principal text, and we base this derivation on [16, 34]. For this, we suppose that we have the following reactions

$$R + 2L \underset{k_-}{\overset{k_+}{\rightleftarrows}} RL_2,$$
$$0 \underset{k_1}{\overset{k_2}{\rightleftarrows}} L. \tag{A1}$$

The first reaction is the binding of 2 ligands L to receptor R in a reversible process to form complex RL_2. We purposely wrote the last reaction because L may be subject to other reactions, and this reaction is a birth–death process that synthesizes and degrades ligands. The stoichiometric coefficients and the stoichiometric matrix are,

$$\alpha_{ij} = \begin{pmatrix} 2 & 1 & 0 \\ 0 & 0 & 1 \\ 0 & 0 & 0 \\ 1 & 0 & 0 \end{pmatrix}, \quad \beta_{ij} = \begin{pmatrix} 0 & 0 & 1 \\ 2 & 1 & 0 \\ 1 & 0 & 0 \\ 0 & 0 & 0 \end{pmatrix}, \quad \Gamma_{ij} = \begin{pmatrix} -2 & 2 & 1 & -1 \\ -1 & 1 & 0 & 0 \\ 1 & -1 & 0 & 0 \end{pmatrix}. \tag{A2}$$

Let L, R, S be the number of molecules of L, R, RL_2 respectively. Thus, the propensity rates are

$$a_1 = k_+ R \frac{L!}{(L-2)!} \frac{1}{\Omega^3}, \qquad a_2 = k_- S \frac{1}{\Omega}, \tag{A3}$$

there is a conservative quantity $R + S = R_0$, the number of initial receptors, then the previous propensities are reduced to

$$a_1 = k_+ (R_0 - S) \frac{L!}{(L-2)!} \frac{1}{\Omega^3}, \qquad a_2 = k_- S \frac{1}{\Omega}, \tag{A4}$$

and

$$\Gamma'_{ij} = \begin{pmatrix} -2 & 2 & 1 & -1 \\ 1 & -1 & 0 & 0 \end{pmatrix}. \tag{A5}$$

If we suppose that the first reactions in (A2) are in the stationary state, S and L are independent, then the central moments between S and L are zero, then we get the next equation

$$\frac{\partial s}{\partial t} = 0 = -k_- s + k_+ (r_0 - s) \frac{1}{\Omega^2} \left\langle \frac{L!}{(L-2)!} \right\rangle, \tag{A6}$$

where $K^2 = \frac{k_-}{k_+}$, $r_0 = R_0/\Omega$, $s = \langle S \rangle / \Omega$ and $r = \langle R \rangle / \Omega$ are the mean concentrations of S and R, from this we get

$$s = r_0 \frac{\frac{1}{\Omega^2} \left\langle \frac{L!}{(L-2)!} \right\rangle}{K^2 + \frac{1}{\Omega^2} \left\langle \frac{L!}{(L-2)!} \right\rangle}. \tag{A7}$$

If we define the Hill function as follows and substitute $r + s = r_0$ and the value of s, we have

$$H = \frac{s}{r+s} = \frac{s}{r_0} = \frac{\frac{1}{\Omega^2} \left\langle \frac{L!}{(L-2)!} \right\rangle}{K^2 + \frac{1}{\Omega^2} \left\langle \frac{L!}{(L-2)!} \right\rangle}, \tag{A8}$$

using the second-moment framework and defined $l = \langle L \rangle / \Omega$ and $M^2_{l,l} = \langle (L - \langle L \rangle)^2 \rangle / \Omega^2$, we get

$$H = \frac{l^2 + M^2_{l,l} - \frac{l}{\Omega}}{K^2 + l^2 + M^2_{l,l} - \frac{l}{\Omega}}. \tag{A9}$$

This expression is exact because we did not make any approximations in the derivation. The derivation presented here is for an activator, but we can perform similar derivations for repressors or only use the relation $D = 1 - H$. For the recovery of the deterministic case, $\Omega \to \infty$ and $M^2_{l,l} = 0$. Following a similar procedure, we can incorporate cases in which the number of ligands that binding the receptor increases.

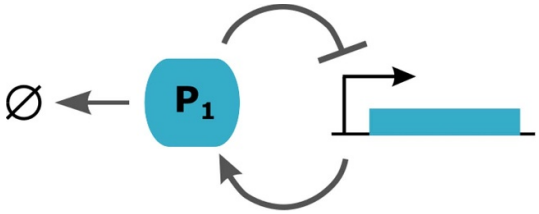

Figure B1. Auto-negative feedback. This is a schematic representation of a gene regulatory network with auto-negative feedback, where protein P_1 suppresses its synthesis, thereby establishing a negative feedback loop. Protein P_1 is degraded.

Appendix B. Third-moment dependence

Following a similar derivation as in the principal text, we construct a set of ODEs that describe the dynamics of a gene regulatory network with auto-negative regulation (see figure B1). In this case, we chose a Hill function as

$$\kappa = \kappa^* \left(\frac{1}{1 + + \left(p_1^3 + 3p_1 M_{1,1}^2 + M_{1,1,1}^3\right) - \frac{3}{\Omega}\left(p_1^2 + M_{1,1}^2\right) + \frac{2p_1}{\Omega^2}} \right), \tag{B1}$$

where p_1, $M_{1,1}^2$ and $M_{1,1,1}^3$ are the mean concentrations, second central moment and third central moment of protein P_1, respectively. In this case the Hill function is for a repressor and depends until the third central moment, we chose the dissociation constant equal to one, $\kappa*$ is the maximum synthesis of the protein, then the set of ODEs that describes the dynamic of the system are

$$\begin{aligned}
\frac{\partial p_1}{\partial t} &= \kappa - \delta_p p_1, \\
\frac{\partial M_{1,1}^2}{\partial t} &= \frac{1}{\Omega}\left(\kappa + \delta_p p_1\right) - 2\delta_p M_{1,1}^2, \\
\frac{\partial M_{1,1,1}^3}{\partial t} &= \frac{1}{\Omega^2}\left(\kappa - \delta_p p_1\right) + \frac{3}{\Omega}\delta_p M_{1,1}^2 + \frac{3M_{1,1}^2}{\Omega}\left(\kappa - \delta_p p_1\right) - 3\delta_p M_{1,1,1}^3.
\end{aligned} \tag{B2}$$

The stationary state of the system is

$$M_{1,1,ss}^2 = \frac{p_{1,ss}}{\Omega}, \qquad M_{1,1,1,ss}^3 = \frac{p_{1,ss}}{\Omega^2}, \tag{B3}$$

and to determine the value of $p_{1,ss}$, it is necessary to solve the next equation

$$0 = \kappa^* \left(\frac{1}{1 + p_{1,ss}^3} \right) - \delta_p p_{1,ss}. \tag{B4}$$

From (B2) we can get a set of ODEs around the equilibrium, for these we define the next,

$$\begin{aligned}
\frac{\partial \kappa}{\partial p_1}\Big|_{\left(p_1 = p_{1,ss}, M_{1,1}^2 = \frac{p_{1,ss}}{\Omega}\right)} &= -\kappa^* \left(3p_{1,ss}\left(p_{1,ss} - \frac{1}{\Omega}\right) + \frac{2}{\Omega^2}\right)\left(\frac{1}{1 + \left(p_{1,ss}\right)^3}\right)^2 \\
&= -p_{1,ss}B_1 + \frac{2B_2}{\Omega^2},
\end{aligned} \tag{B5}$$

$$\frac{\partial \kappa}{\partial M_{1,1}^2}|_{\left(p_1=p_{1,ss},M_{1,1}^2=\frac{p_{1,ss}}{\Omega}\right)} = -\kappa^* 3\left(p_{1,ss}-\frac{1}{\Omega}\right)\left(\frac{1}{1+(p_{2,ss})^3}\right)^2 = -B_1,$$
$$\frac{\partial \kappa}{\partial M_{1,1,1}^2}|_{\left(p_1=p_{1,ss},M_{1,1}^2=\frac{p_{1,ss}}{\Omega}\right)} = -\kappa^*\left(\frac{1}{1+(p_{2,ss})^3}\right)^2 = -B_2. \tag{B6}$$

Now we define the next values $\Delta p_1 = p_1 - p_{1,ss}$, $\Delta M_{1,1}^2 = M_{1,1}^2 - M_{1,1,ss}^2 \Delta M_{1,1}^2 = M_{1,1}^2 - M_{1,1,ss}^2$ and $\Delta M_{1,1,1}^3 = M_{1,1,1}^3 - M_{1,1,1,ss}^3$, then the set of ODEs around the equilibrium became like follow,

$$\begin{aligned}
\frac{\partial \Delta p_1}{\partial t} &= \left(-p_{1,ss}B_1 + \frac{2B_2}{\Omega^2} - \delta_p\right)\Delta p_1 - B_1\Delta M_{1,1}^2 - B_2\Delta M_{1,1,1}^3,\\
\frac{\partial \Delta M_{1,1}^2}{\partial t} &= \frac{1}{\Omega}\left(-p_{1,ss}B_1 + \frac{2B_2}{\Omega^2} + \delta_p\right)\Delta p_1 - \left(\frac{B_1}{\Omega} + 2\delta_p\right)\Delta M_{1,1}^2 - \frac{B_2}{\Omega}\Delta M_{1,1,1}^3,\\
\frac{\partial \Delta M_{1,1,1}^3}{\partial t} &= \left(\frac{1}{\Omega^2} + \frac{3M_{1,1,ss}^2}{\Omega}\right)\left(-p_{1,ss}B_1 + \frac{2B_2}{\Omega^2} - \delta_p\right)\Delta p_1\\
&\quad - \left(\frac{B_1}{\Omega}\left(\frac{1}{\Omega} + 3M_{1,1,ss}^2\right) + \frac{3\delta_p}{\Omega}\right)\Delta M_{1,1}^2 - \left(\frac{B_2}{\Omega^2} + 3\delta_p\right)\Delta M_{1,1,1}^3,
\end{aligned} \tag{B7}$$

using these equations, we determine the Jacobian matrix and calculate the eigenvalues of the system.

Appendix C. Stochastic simulations

To compare the results from the analytical model for a negative regulation that is present in this work, we performed a stochastic simulation of the system, but we considered all reactions, including those that come from the derivation of the Hill function; for this, we have the following reactions that are given in [16],

$$\left|\begin{array}{c} 2P_2 + R_1 \xrightarrow{k_1^+} R_1^* \\ R_1 \xrightarrow{\gamma_1^*} R_1 + P_1 \\ P_1 \xrightarrow{\delta_1} \emptyset \end{array}\right| \left|\begin{array}{c} 2P_1 + R_2^* \xrightarrow{k_1^+} R_2 \\ R_2 \xrightarrow{\gamma_2^*} R_2 + P_2 \\ P_2 \xrightarrow{\delta_2} \emptyset \end{array}\right|$$

R_1, R_1^*, and P_1 are the active polymerase region, inactive polymerase region, and protein, respectively, similar to the other variables. For the left hand, the first reaction is the union of protein 1 to the active polymerase to inactivate the polymerase, the next is the synthesis of the protein from an active polymerase, and the last is the degradation of the protein, which is similar to the right hand, but here protein 1 activates the polymerase region.

The stoichiometric coefficients are α_{li} and β_{li}, and the stoichiometric matrix Γ_{il} are,

$$\alpha_{li} = \begin{pmatrix} 1 & 0 & 0 & 0 & 0 & 2 \\ 0 & 1 & 0 & 0 & 0 & 0 \\ 1 & 0 & 0 & 0 & 0 & 0 \\ 0 & 0 & 1 & 0 & 0 & 0 \\ 0 & 0 & 2 & 0 & 1 & 0 \\ 0 & 0 & 0 & 1 & 0 & 0 \\ 0 & 0 & 0 & 1 & 0 & 0 \\ 0 & 0 & 0 & 0 & 0 & 1 \end{pmatrix}, \quad \beta_{li} = \begin{pmatrix} 0 & 1 & 0 & 0 & 0 & 0 \\ 1 & 0 & 0 & 0 & 0 & 2 \\ 1 & 0 & 1 & 0 & 0 & 0 \\ 0 & 0 & 0 & 0 & 0 & 0 \\ 0 & 0 & 0 & 1 & 0 & 0 \\ 0 & 0 & 2 & 0 & 1 & 0 \\ 0 & 0 & 0 & 1 & 0 & 1 \\ 0 & 0 & 0 & 0 & 0 & 0 \end{pmatrix}, \tag{C1}$$

$$\Gamma_{il} = \begin{pmatrix} -1 & 1 & 0 & 0 & 0 & 0 & 0 & 0 \\ 1 & -1 & 0 & 0 & 0 & 0 & 0 & 0 \\ 0 & 0 & 1 & -1 & -2 & 2 & 0 & 0 \\ 0 & 0 & 0 & 0 & 1 & -1 & 0 & 0 \\ 0 & 0 & 0 & 0 & -1 & 1 & 0 & 0 \\ -2 & 2 & 0 & 0 & 0 & 0 & 1 & -1 \end{pmatrix}. \tag{C2}$$

The propensity rates of the system,

$$a_1 = k_1^+ R_1 \frac{P_2(P_2-1)}{\Omega^3}, \qquad a_5 = k_2^+ R_2^* \frac{P_1(P_1-1)}{\Omega^3},$$
$$a_2 = k_1^- \frac{R_1^*}{\Omega}, \qquad a_6 = k_2^- \frac{R_2}{\Omega}.$$

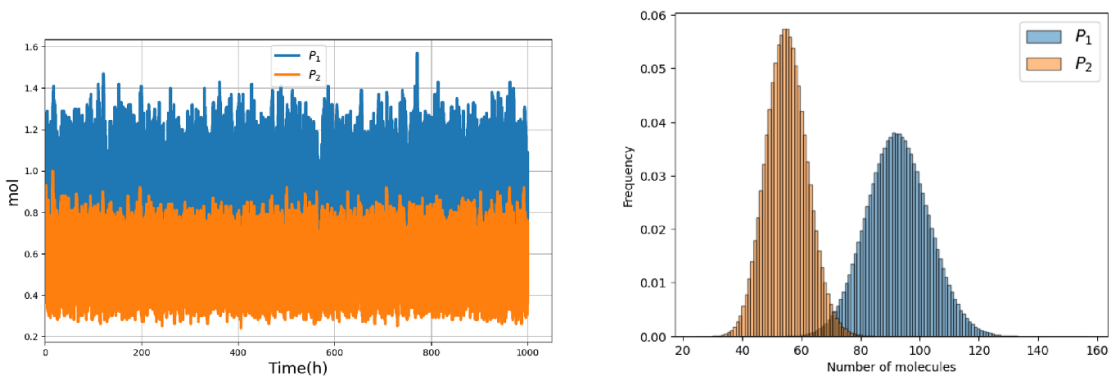

Figure C1. Stochastic simulation of a negative feedback. The result of the stochastic simulation of the system, where we used the parameters and initial conditions of table D3. On the left is the stochastic simulation, and on the right is the histogram of the number of protein molecules.

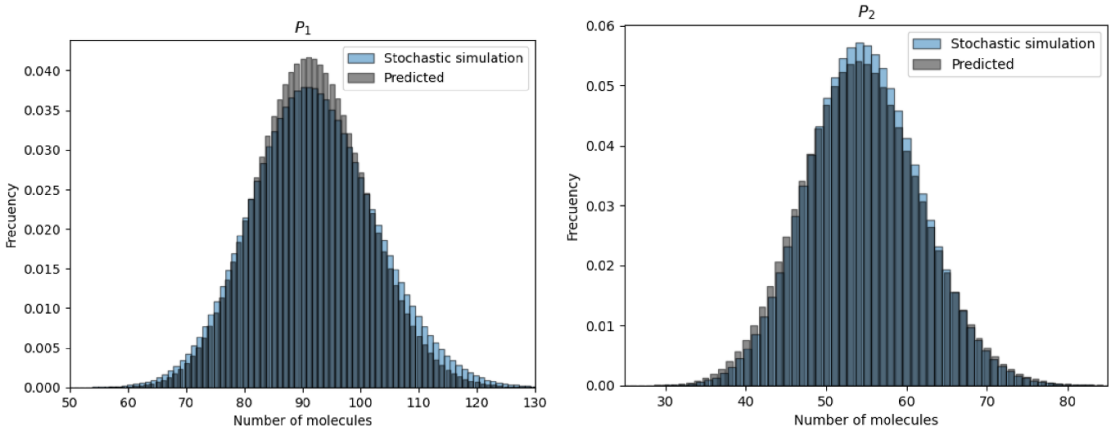

Figure C2. Comparing distributions. We compare the distribution obtained from the stochastic simulations with that predicted by equation (17). On the left, we have protein P_1 and on the right, protein P_2. We can see that the values between the predicted and stochastic simulations have a similar form.

$$a_3 = \gamma_1^* \frac{R_1}{\Omega}, \qquad a_7 = \gamma_2^* \frac{R_2}{\Omega},$$
$$a_4 = \delta_1 \frac{P_1}{\Omega}, \qquad a_8 = \delta_2 \frac{P_2}{\Omega}. \tag{C3}$$

Using all of these elements, we made a stochastic simulation following the Gillespie algorithm; the results are in figure C1. Where we plotted the stochastic simulations and the histograms of the number of molecules of the proteins P_1 and P_2.

In equations (17), the model predicts that the stationary distributions for each protein are Poisson distributions. To validate this, we compared the results of the stochastic simulations with those for each protein, as shown in figure C2. Here, we can see that the distribution obtained by the stochastic simulations and the one predicted by each protein in the stationary state has a similar form. The difference arises from the fact that the prediction is exclusively in the stationary state, whereas in the stochastic simulations, there are still dynamics.

Appendix D. Parameters

Tables D1–D3 list the parameters and initial conditions of the proposed model presented in this study. We also use the same parameters for the deterministic and stochastic models, because they have a similar structure, but in the deterministic model, we do not consider the dynamics of the variance $M_{i,i}^2$ ($i \in (1,2)$) and $A_3 = A_4 = 0$.

Table D1. Parameters and initial conditions for the system. ($i \in 1, 2$) In this table, we show the parameters and initial conditions used for the gene network with negative feedback in a region with damped oscillations.

Parameters	Description	Value
A_1	P_1 synthesis rate by P_2.	$2\ h^{-1}$
A_2	P_1 synthesis rate by P_1.	$2\ h^{-1}$
A_3	P_2 synthesis rate.	$1\ h^{-1}$
A_4	P_2 synthesis rate.	$1\ h^{-1}$
δ	P_1 degradation rate.	$0.1\ h^{-1}$
$\Delta p_1(0)$	Initial mean concentration of Δp_1.	0 mol
$\Delta p_2(0)$	Initial mean concentration of Δp_2.	0.1 mol
$\Delta M^2_{i,i}(0)$	Initial second central moment of concentration of species.	$0\ mol^2$

Table D2. Parameters and initial conditions for the system. ($i \in 1, 2$) In this table, we show the parameters and initial conditions used for the gene network with negative feedback in a region with a stable point.

Parameters	Description	Value
A_1	P_1 synthesis rate by P_2.	$2\ h^{-1}$
A_2	P_1 synthesis rate by P_1.	$2\ h^{-1}$
A_3	P_2 synthesis rate.	$1\ h^{-1}$
A_4	P_2 synthesis rate.	$1\ h^{-1}$
δ	P_1 degradation rate.	$3.5\ h^{-1}$
$\Delta p_1(0)$	Initial mean concentration of Δp_1.	0 mol
$\Delta p_2(0)$	Initial mean concentration of Δp_2.	0.1 mol
$\Delta M^2_{i,i}(0)$	Initial second central moment of concentration of species.	$0\ mol^2$

Table D3. Parameters and initial conditions for the stochastic simulation. In this table, we show the parameters and initial conditions used for the gene network with negative feedback.

Parameters	Description	Value
k_1^+	Rate of binding of R_1 and P_2.	$\epsilon^{-1}\,(mol^2 \times h)^{-1}$
k_1^-	Rate of decoupling.	$\epsilon^{-1}\,h^{-1}$
k_2^+	Rate of binding of R_2^* and P_1.	$\epsilon^{-1}\,(mol^2 \times h)^{-1}$
k_2^-	Rate of decoupling.	$\epsilon^{-1}\,h^{-1}$
ϵ	Inverse velocity to reach the stationary state.	0.005
γ_1^*	P_1 synthesis rate.	$4\ h^{-1}$
γ_2^*	P_2 synthesis rate.	$1\ h^{-1}$
δ_1	P_1 degradation rate.	$1\ h^{-1}$
δ_2	P_1 degradation rate.	$1\ h^{-1}$
$R_1(0)$	Initial number of molecules R_1.	$0.6\ \Omega$
$R_1^*(0)$	Initial number of molecules R_1^*.	$0.4\ \Omega$
$P_1(0)$	Initial number of molecules P_1.	$0.91\ \Omega$
$R_2(0)$	Initial number of molecules R_2.	$0.2\ \Omega$
$R_2^*(0)$	Initial number of molecules R_2^*.	$0.8\ \Omega$
$P_2(0)$	Initial number of molecules P_2.	$0.54\ \Omega$
Ω	Size of the system.	100

References

[1] Alon U 2019 *An Introduction to Systems Biology: Design Principles of Biological Circuits* (CRC Press)

[2] Raser J M and O'Shea E K 2005 Noise in gene expression: origins, consequences and control *Science* **309** 2010–3

[3] Gardiner C 2009 *Stochastic Methods* vol 4 (Springer)

[4] Hernández-García M E, Gómez-Schiavon M and Velázquez-Castro J 2024 Extrinsic fluctuations in the p^{53} cycle *J. Chem. Phys.* **161** 18

[5] Biondo M, Singh A, Caselle M and Osella M 2023 Out-of-equilibrium gene expression fluctuations in the presence of extrinsic noise *Phys. Biol.* **20** 056007

[6] Eldar A and Elowitz M B 2010 Functional roles for noise in genetic circuits *Nature* **467** 167–73

[7] Gillespie D T 2000 The chemical Langevin equation *J. Chem. Phys.* **113** 297–306

[8] Thomas P, Matuschek H and Grima R 2013 How reliable is the linear noise approximation of gene regulatory networks? *BMC Genomics* **14** 1–15

[9] El-Samad H and Khammash M 2006 Regulated degradation is a mechanism for suppressing stochastic fluctuations in gene regulatory networks *Biophys. J.* **90** 3749–61

[10] Bokes P and Singh A 2019 Controlling noisy expression through auto regulation of burst frequency and protein stability *Proc. Int. Workshop Hybrid Syst. Biol* (Springer) pp 80–97

[11] Zhang Z, Nieto C and Singh A 2023 Comparing negative feedback mechanisms in gene expression: from single cells to cell populations *Proc. 62nd IEEE Conf. Decis. Control (CDC)* pp 3744–9

[12] Gómez-Schiavon M, Montejano-Montelongo I, Orozco-Ruiz F S and Sotomayor-Vivas C 2024 The art of modeling gene regulatory circuits *npj Syst. Biol. Appl.* **10** 60

[13] Gomez-Uribe C A and Verghese G C 2007 Mass fluctuation kinetics: capturing stochastic effects in systems of chemical reactions through coupled mean-variance computations *J. Chem. Phys.* **126** 024109
[14] Fröhlich F, Thomas P, Kazeroonian A, Theis F J, Grima R and Hasenauer J 2016 Inference for stochastic chemical kinetics using moment equations and system size expansion *PLoS Comput. Biol.* **12** e1005030
[15] Hernández-García M E, Moreno-Barbosa E and Velázquez-Castro J 2025 An exact moment-based approach for chemical reaction-diffusion networks: from mass action to Hill functions (arXiv:2505.09053)
[16] Hernández-García M E and Velázquez-Castro J 2023 Corrected Hill function in stochastic gene regulatory networks (arXiv:2307.03057)
[17] Ale A, Kirk P and Stumpf M P H 2013 A general moment expansion method for stochastic kinetic models *J. Chem. Phys.* **138** 17
[18] El Samad H and Khammash M 2004 Stochastic stability and its application to the analysis of gene regulatory networks *Proc. 43rd IEEE Conf. Decis. Control* vol 3 3001–6
[19] Jiao T, Zong G, Nguang S K and Zhang C 2018 Stability analysis of genetic regulatory networks with general random disturbances *IEEE Trans. NanoBiosci.* **18** 128–36
[20] Sun Y, Feng G and Cao J 2012 Robust stochastic stability analysis of genetic regulatory networks with disturbance attenuation *Neurocomputing* **79** 39–49
[21] Smadbeck P and Kaznessis Y N 2015 On a theory of stability for nonlinear stochastic chemical reaction networks *J. Chem. Phys.* **142** 184101–12
[22] Ghusinga K R, Vargas-Garcia C A, Lamperski A and Singh A 2017 Exact lower and upper bounds on stationary moments in stochastic biochemical systems *Phys. Biol.* **14** 04LT01
[23] Sayama H 2015 *Introduction to the Modeling and Analysis of Complex Systems* (Open SUNY Textbooks)
[24] Hancock E J, Ang J, Papachristodoulou A and Stan G B 2017 The interplay between feedback and buffering in cellular homeostasis *Cell Syst.* **5** 498–508
[25] Xiao M and Cao J 2008 Genetic oscillation deduced from Hopf bifurcation in a genetic regulatory network with delays *Math. Biosci.* **215** 55–63
[26] Takada M, Hori Y, Hara S 2012 Existence of oscillations in cyclic gene regulatory networks with time delay (arXiv:1212.6325)
[27] Lev Bar-Or R, Maya R, Segel L A, Alon U, Levine A J and Oren M 2000 Generation of oscillations by the p^{53}-Mdm2 feedback loop: a theoretical and experimental study *Proc. Natl. Acad. Sci.* **97** 11250–5
[28] Hirata H, Yoshiura S, Ohtsuka T, Bessho Y, Harada T, Yoshikawa K and Kageyama R 2002 Oscillatory expression of the bHLH factor Hes1 regulated by a negative feedback loop *Science* **298** 840–3
[29] Liu Z H, Dai X M and Du B 2015 Hes1: a key role in stemness, metastasis and multidrug resistance *Cancer Biol. Ther.* **16** 353–9
[30] Marciano D C, Lua R C, Katsonis P, Amin S R, Herman C and Lichtarge O 2014 Negative feedback in genetic circuits confers evolutionary resilience and capacitance *Cell Rep.* **7** 1789–95
[31] Smeenk L *et al* 2008 Characterization of genome-wide p^{53}-binding sites upon stress response *Nucleic Acids Res.* **36** 3639–54
[32] Baroni T E *et al* 2004 A global suppressor motif for p^{53} cancer mutants *Proc. Natl. Acad. Sci.* **101** 4930–5
[33] Kumar N, Platini T and Kulkarni R V 2014 Exact distributions for stochastic gene expression models with bursting and feedback *Phys. Rev. Lett.* **113** 268105
[34] Hernández-García M E and Velázquez-Castro J 2025 Relationship between decimal Hill coefficient, intermediate processes and mesoscopic fluctuations in gene expression *ACS Omega* **10** 13906–14
[35] Van Kampen N G 1976 The expansion of the master equation *Advances in Chemical Physics* **34** 245–309